AGU100 ADVANCING EARTH AND SPACE SCIENCE

Geophysical Research Letters

RESEARCH LETTER
10.1029/2018GL078770

Key Points:
- The surface temperature in the 20th century at Styx Glacier (western coast of the Ross Sea) is higher by 1.7 +/− 0.4 degrees than before 1900 CE
- No clear warming trend since the mid-20th century was found in northern Victoria Land, Antarctica
- The climate over the western coast of the Ross Sea might be affected by the Southern Hemisphere Annular Mode

Supporting Information:
- Supporting Information S1
- Data Set S1

Correspondence to:
J. Ahn,
jinhoahn@snu.ac.kr

Citation:
Yang, J.-W., Han, Y., Orsi, A. J., Kim, S.-J., Han, H., Ryu, Y., et al. (2018). Surface temperature in twentieth century at the Styx Glacier, northern Victoria Land, Antarctica, from borehole thermometry. *Geophysical Research Letters, 45*, 9834–9842. https://doi.org/10.1029/2018GL078770

Received 2 JUN 2018
Accepted 29 AUG 2018
Accepted article online 4 SEP 2018
Published online 22 SEP 2018

Surface Temperature in Twentieth Century at the Styx Glacier, Northern Victoria Land, Antarctica, From Borehole Thermometry

Ji-Woong Yang[1], Yeongcheol Han[2], Anaïs J. Orsi[3], Seong-Joong Kim[2], Hyangsun Han[2], Yeongjun Ryu[1], Youngjoon Jang[1], Jangil Moon[2], Taejin Choi[2], Soon Do Hur[2], and Jinho Ahn[1]

[1]School of Earth and Environmental Sciences, Seoul National University, Seoul, South Korea, [2]Korea Polar Research Institute, Incheon, South Korea, [3]Laboratoire des Sciences du Climat et de l'Environnement, LSCE/IPSL, CEA-CNRS-UVSQ, Université Paris-Saclay, l'Orme des merisiers, Gif-sur-Yvette, France

Abstract Reconstruction of the long-term surface temperature history in Antarctica is important for a better understanding of human-induced climate changes, especially since the Industrial Revolution. We present here a surface temperature history spanning the last century at Styx Glacier, located on the eastern coast of northern Victoria Land, which is reconstructed using borehole logging data. Our results indicate that surface temperatures in the 20th century were 1.7 ± 0.4 °C higher than the long term averages over 1600–1900 Common Era, indicating regional warming over the eastern coast of northern Victoria Land. However, we found no evidence for significant warming across the northern Victoria Land since the mid-20th century. A global reanalysis as well as the reconstruction of proxy records demonstrate that the climate in this region was more affected by changes in the Southern Hemisphere Annular Mode than in the Amundsen-Bellingshausen Sea Low.

Plain Language Summary The western coast of the Ross Sea, northern Victoria Land, is one of several regions around the world where the temperature history is highly uncertain. Here we provide a temperature reconstruction using borehole logging data from Styx Glacier. The reconstructed temperature history indicates that the surface temperature at Styx Glacier in the 20th century is higher than in previous centuries, although there is no significant trend since ~1950s. The lack of recent warming trend off the western Ross Sea is in contrast to the warming in the Antarctic Peninsula and West Antarctica.

1. Introduction

Understanding the mechanisms of Antarctic climate change is crucial for future projections of sea-level rise, sea ice change, ocean circulations, and consequently, future global climate (Collins et al., 2013). Previous surface temperature reconstructions over Antarctica found inhomogeneous recent warming trends since 1958 Common Era (CE), showing a strong warming in the Antarctic Peninsula (AP) and West Antarctica (WA), but an insignificant overall warming over East Antarctica (EA; e.g., Nicholas & Bromwich, 2014; Stieg et al., 2009), although local warming has been observed in some parts of EA (Muto et al., 2011). The significant recent warming trends over AP and WA were confirmed by borehole temperature inversions (Barrett et al., 2009; Orsi et al., 2012; Zagorodnov et al., 2012).

The warming in the AP since the late 1970s has been attributed to the positive phase of the Southern Hemisphere Annular Mode (SAM), which is the leading mode of climate variability in the Southern Hemisphere that can be defined by differences in sea level pressure between middle and high latitudes (e.g., Marshall, 2003). The recent SAM increase is due to stratospheric ozone depletion during summer (Thompson et al., 2011) and strong teleconnections with the tropics (e.g., Schneider et al., 2012). On the other hand, the WA warming has been largely attributed to the strengthening of northerly warm meridional winds caused by changes in the central pressure and mean position of the Amundsen Bellingshausen Sea Low (ASL), a persistent low pressure centered over the Amundsen-Bellingshausen Sea and the Ross Sea (Hosking et al., 2013, 2016), which is forced by tropical sea surface temperatures (e.g., Fogt & Wovrosh, 2015).

The Earth's mean surface temperature has substantially increased due to human activity especially since the Industrial Revolution. However, the current temporal coverage of temperature observation data is insufficient

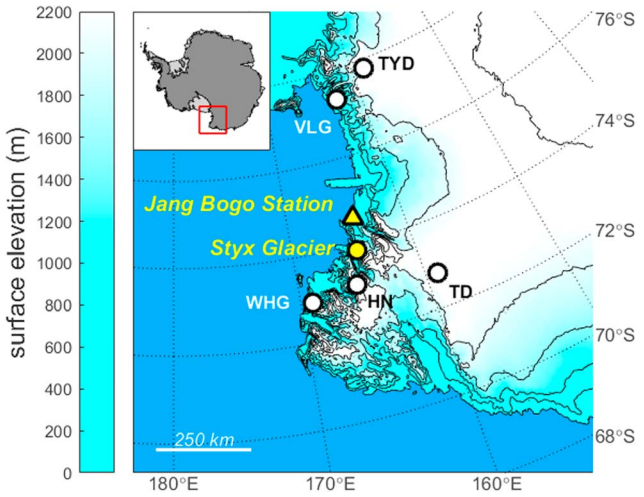

Figure 1. The locations of the Styx Glacier along with previous ice core sites on the western coast of the Ross Sea (HN = Hercules Névé; TD = Talos Dome; TYD = Taylor Dome; WHG = Whitehall Glacier; VLG = Victoria Lower Glacier). The color bar indicate the surface elevation based on the Bedmap2 data set (Fretwell et al., 2013). This map was created using the Antarctic Mapping Tool (Greene et al., 2017).

for evaluating anthropogenic warming in Antarctica. Improving the spatial coverage of long-term temperature reconstructions is particularly important for a better understanding of regional climate changes in Antarctica. The Ross Sea is the region of bottom water formation (Jacobs, 2004), the highest biological production (Arrigo & van Dijken, 2003), and the highest increase in sea-ice extent (Comiso et al., 2017; Sinclair et al., 2014). However, due to the complex topography and relatively low temporal resolution of observations, the reanalysis-based temperature fields show lower reconstruction skill in the western coast of the Ross Sea than in the interior EA (Nicholas & Bromwich, 2014). Existing past temperature (T) reconstructions in this region have relied exclusively on stable isotope paleothermometry ($\delta^{18}O_{ice}$), but the slope of $\delta^{18}O_{ice}/T$ is not spatially or temporally constant (e.g., Goursaud et al., 2018), and it is rarely constrained in mountainous areas. These limitations make accurate temperature reconstruction difficult. In this study, we present an independent surface temperature history in the western coast of the Ross Sea using borehole temperature measurements from Styx Glacier, northern Victoria Land.

2. Materials and Methods

2.1. Styx Glacier Borehole Temperature Logging

Styx Glacier (73°51.10′S, 163°41.22′E, 1,623 m above sea level) is located near the western coast of the Ross Sea, northern Victoria Land (Figure 1). A shallow (depth of 210.5 m) ice core was drilled during the 2014–2015 austral summer (Han et al., 2015). The drilling site is close to the ice divide, and the horizontal ice flow was estimated as ~0.9 m/year by interferometric synthetic aperture radar observations (supporting information Figure S2). Ground penetrating radar survey showed that the ice thickness at drilling location is 550 m (Hur, 2013). The temperature of the 210.5-m borehole was measured in November 2016, 2 years after drilling. The borehole temperature was logged twice in both downward and upward directions. The logging interval was every 1 m for the upper 15 m and every 3 m down to 90 m; 5 m intervals were used for depths below 90 m. The thermistor was held in place for at least 10 min to allow it to stabilize, and the resistance was averaged for 5 min. The measured resistance data were converted to temperature by an extended Steinhart-Hart calibration function (Clow et al., 1996). The expanded absolute accuracy of our logging device is 0.1 K in the range of 0 to −35 °C (Institute of Calibration & Technology Co., Ltd.). The relative accuracy of the borehole logging data is 9 mK, which is estimated as a pooled standard deviation of the four repeated temperature measurements. We note that the relative temperature difference between the depth intervals is more important for the borehole temperature inversion than the absolute temperature (Orsi et al., 2012).

2.2. Temperature Reconstruction

We used a one-dimensional ice and heat flow model (forward model) and least-square technique (inversion model) to reconstruct the temperature history. Here we assume that the horizontal heat advection is negligible due to a low horizontal velocity (Figure S2). The details on the temperature reconstruction method and uncertainty estimates are explained in Orsi et al. (2012, 2014, 2017). The parameters used in the inversion scheme are detailed in Section S3.

The firn and ice bulk densities were measured on site during the drilling campaign (Han et al., 2015). The snow accumulation rate was determined by the annual layer thickness calculated from the ice chronology, bulk density profile, and thinning function. We first determined the gas chronology based on methane correlation (Blunier et al., 2007; Buizert et al., 2015) with West Antarctic Ice Sheet (WAIS) Divide records (Mitchell et al., 2011, 2013), which was then converted to ice age scale by using the gas age-ice age difference at the lock-in depth (52.8 m). The gas and ice ages at lock-in depth were dated by carbon dioxide (CO_2) mixing ratio of firn air and the Herron-Langway empirical firn densification model (Herron & Langway, 1980), respectively. The thinning function was calculated by Nye (1963) and Dansgaard-Johnsen model (Dansgaard & Johnsen, 1969). Details on the snow accumulation rate estimation are described in Supporting Information S1.

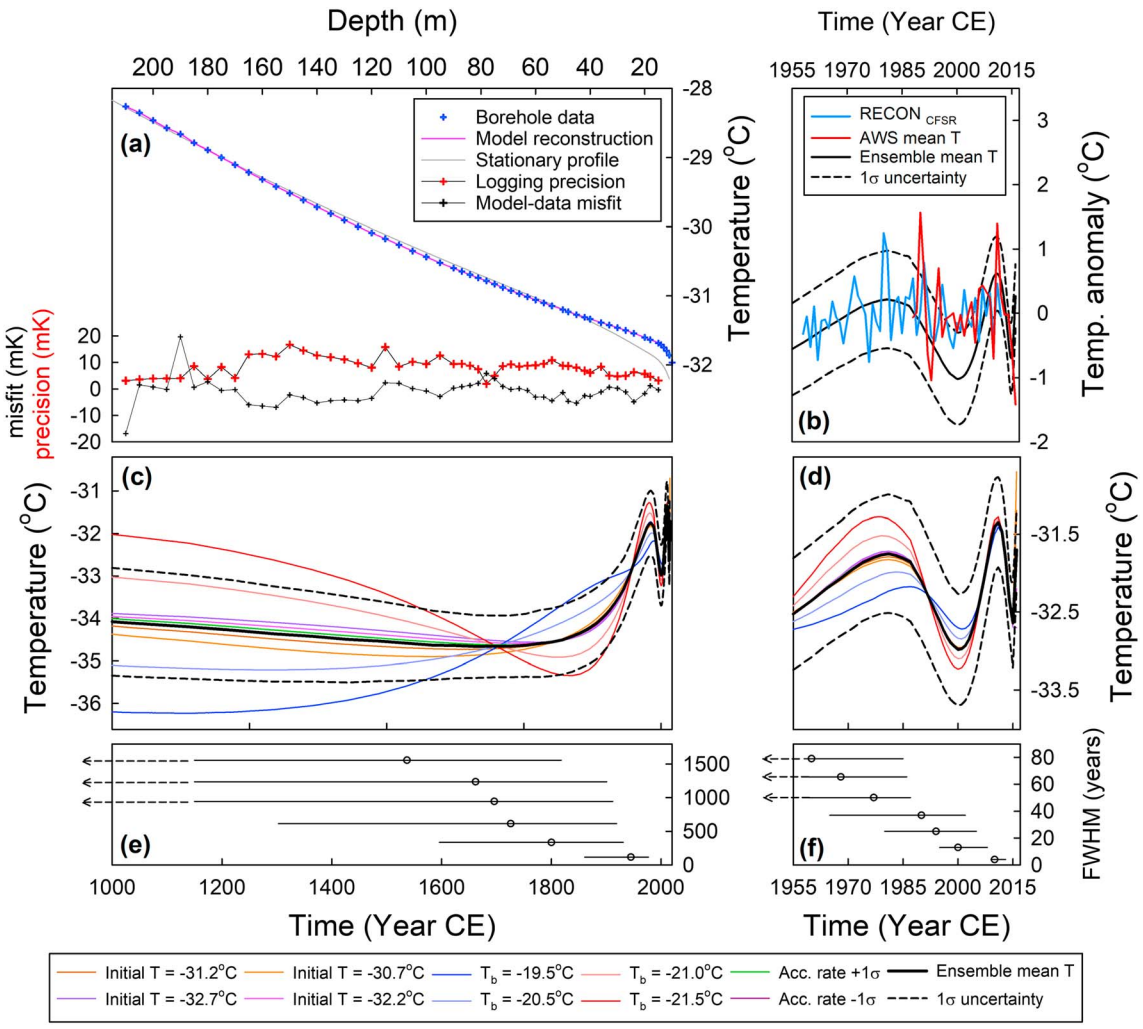

Figure 2. Model fit, sensitivity tests, and smoothing windows of Styx Glacier temperature reconstructions. (a; Upper) Comparison of borehole logging data (blue crosses) with the model reconstructed temperature profile (solid magenta line), along with the stationary temperature profile (gray, −31.7 °C for 15,000-year run). (a; Lower) The precision of borehole logging data (red crosses), and model-data misfit (black crosses). (b) Comparison of Styx Glacier temperature anomalies (relative to the 1960–1990 CE period) with reanalysis-based reconstructions (blue, $RECON_{CFSR}$) and the average of the mean annual temperature from the automated weather system (AWS; red, see text). (c) Results of sensitivity tests for 1000–2010 CE. The ensemble mean and 1 standard deviation (1σ) ranges are plotted in black solid and dashed lines, respectively. (d) Same as (c) but enlarged for 1955–2016 CE. (e) Smoothing windows at selected time steps (black open circles) are indicated as full widths at half maximum (FWHM). (f) Same as (e) but for the 1955–2016 CE interval. CE = Common Era.

The forward model was initialized with a constant climate history with a seasonal temperature cycle (Figure S9). The stationary temperature profile for the initial condition was obtained after a 15,000-year model run. The mean annual temperature of −32.5 °C, basal temperature of −20.5 °C, and basal temperature gradient of 0.0221 °C/m were chosen to yield a temperature profile close to the borehole logging data. Styx Glacier is situated in the Melbourne volcanic province, which may cause higher basal heat flux than other regions. The indirect estimates from seismic model (Shapiro & Ritzwoller, 2004) and satellite observation (Maule et al., 2005) show a larger heat flux than used in our calculation. However, changes in basal heat flux do not cause significant changes to the model calculations (see Supporting Information S1 for the sensitivity tests).

2.3. Sensitivity Tests

We carried out sensitivity tests to see which parameters strongly influenced the temperature reconstructions and to conservatively define the uncertainty ranges. The sensitivity tests revealed that the temperature history was the most sensitive to the initial temperature (T_0) and basal temperature (T_b). We created an

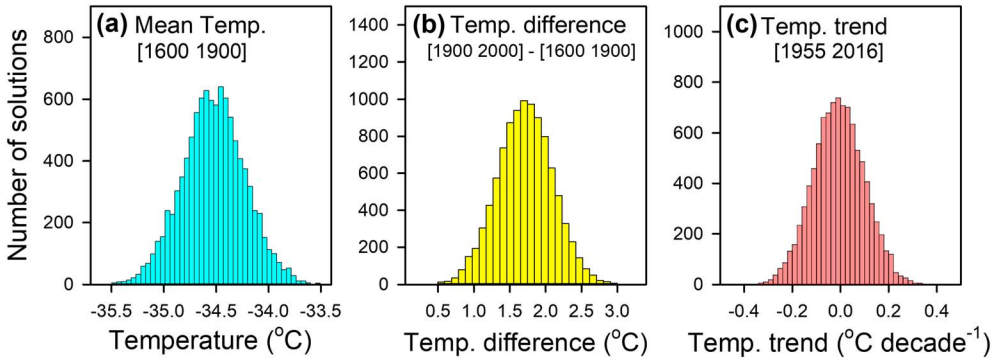

Figure 3. (a) Histogram of the mean temperature over 1600–1900 CE. (b) Histogram of the temperature difference between the long term mean and the 20th century; the results indicate that the 20th century was 1.7 ± 0.4 °C warmer than the long term 1600–1900 CE average. (c) Histogram of the temperature trend over the 1955–2016 CE interval shows a negligible trend of −0.01 ± 0.11 °C per decade. CE = Common Era.

ensemble of eight scenarios of ±0.5 and ±1.0 °C cases for the initial temperature and basal temperature, and we added two cases of ±1σ of snow accumulation rate history to account for heat advection. Figure 2c shows the temperature history of each sensitivity test and the mean ensemble temperature with its 1σ range. Also plotted in Figure 2 are smoothing windows in full widths at half maximum of the smoothing function at selected time steps. Given that the smoothing windows earlier than around 1700 CE were over 1,000 years and that the sensitivity results diverged substantially, there was no reconstruction skill for centennial temperature changes before around 18th century.

3. Results

3.1. Styx Glacier Temperature History

The reconstructed surface temperature history at Styx Glacier exhibits an increase from the 17–19th to 20th century, which has paused in the mid-1950s (Figures 2c and 2d). As the smoothing windows exceed 200 years at 1900 CE, our inversion result provides a long-term average temperature for older period (Figure 2e). The mean temperature over 1600–1900 CE was −34.5 ± 0.3 °C (Figure 3a). The surface temperature at Styx Glacier increased by ~1.7 ± 0.4 °C from the mean over the 17–19th centuries to the 20th century (Figure 3b). However, this warming is not clearly observed in the $\delta^{18}O$-based regional temperature reconstruction over the Victoria Land Coast from Antarctic-2k framework of Past Global Changes project (Stenni et al., 2017; Figure 4a). It shows a warming of 0.5 °C in the intervals between 1600–1900 CE and 1900–2000 CE. We should note that the Antarctic-2k record is a spatially averaged temperature reconstruction over the Victoria Land Coast region, which is composed of the northernmost Victoria Land, the western coast of the Ross Sea, and the western part of the Ross Ice Shelf (Stenni et al., 2017). Therefore, if warming across the Victoria Land Coast since the 19th century is not consistent, then only a moderate warming signal would appear in the averaged regional temperature. Figure 4b compares the temperature at the Styx Glacier with the stable isotope ratios ($\delta^{18}O_{ice}$ and δD_{ice}) from ice cores located in northern Victoria Land. We found no warming trend since 1600 CE in Talos Dome (TALDICE and TD96 cores), located on the inland plateau, ~250 km from the Ross Sea (Stenni et al., 2002). In contrast, the $\delta^{18}O_{ice}$ records at Hercules Névé, located near the eastern coast of northern Victoria Land (Figure 1), show an increase from around the 19th century to the mid-20th century. At Hercules Névé, the mean difference of $\delta^{18}O_{ice}$ between the intervals of 1770–1899 CE and 1900–1992 CE is 1.4‰, which is equivalent to a warming of 1.1 ± 0.1 °C assuming the $\delta^{18}O_{ice}/T$ slope of 0.83 ± 0.05‰/°C calculated from the European Centre Hamburg Model (ECHAM) simulation over the Victoria Land Coast (Stenni et al., 2017). This indicates that warming from the 17–19th centuries to the 20th century was probably confined to the coastal region of northern Victoria Land.

The warming trend found from the 17–19th centuries to the 20th century weakened after the mid-20th century (Figure 4a). The Styx Glacier temperature trend calculated from the average of linear regression slopes of the 10,000 solutions over the [t, 2016] (t = 1800, 1801, …, 2015) interval became statistically insignificant ($p > 0.05$) after 1955 CE (Figure 3c). This is in contrast to WA and AP, where the borehole temperatures

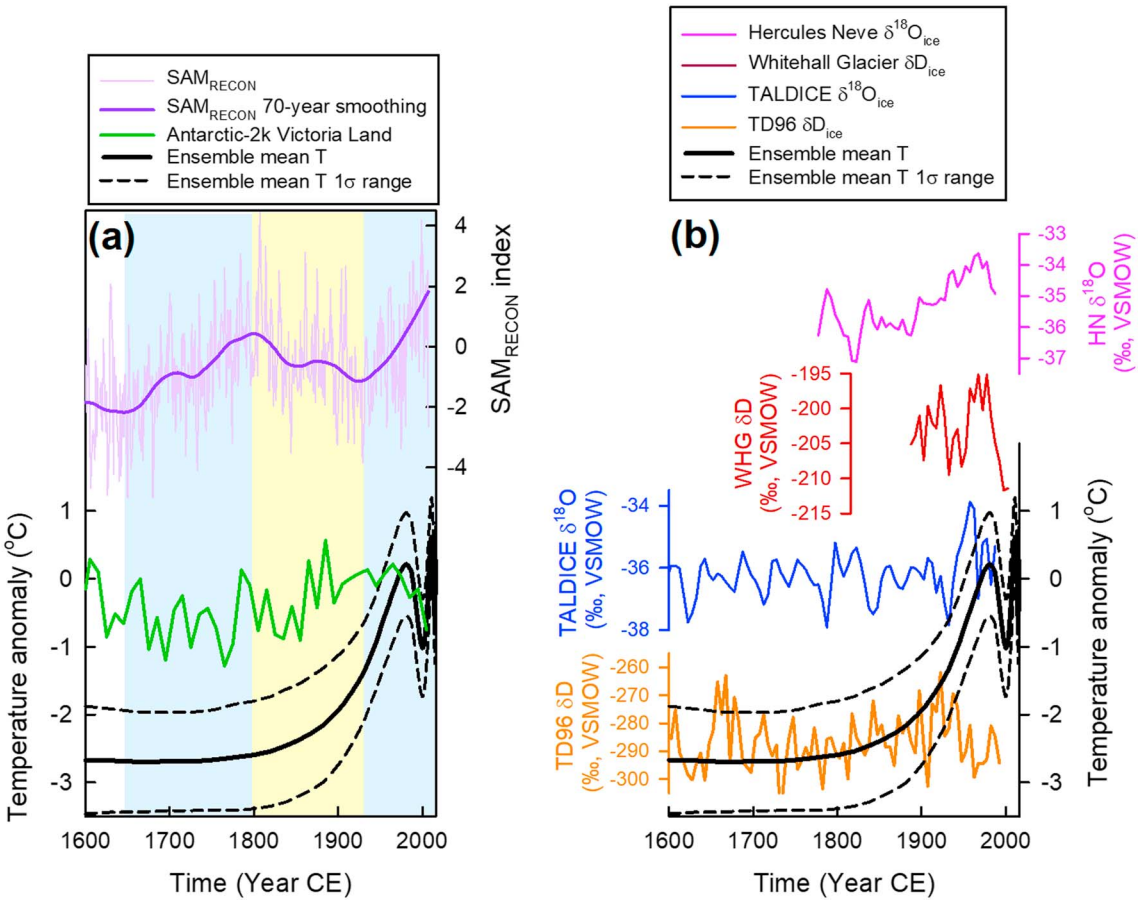

Figure 4. (a) Comparison between the reconstructed SAM index (thin purple, SAM_{RECON}; Abram et al., 2014) and Styx Glacier temperatures since the 17th century. Also plotted are the 70-year-smoothed SAM_{RECON} record (thick dark purple), the Styx Glacier temperature anomalies relative to the 1960–1990 CE average (black), and the Antarctic-2k temperature reconstructions in 10-year bins scaled by ECHAM results (green; Stenni et al., 2017). The yellow and blue shadings denote the period when SAM_{RECON} shows negative and positive slope, respectively. (b) Comparison between the Styx Glacier temperature anomaly (black) and the stable isotope ratios ($\delta^{18}O_{ice}$ and δD_{ice}) from Hercules Névé (pink, Stenni et al., 1999), Whitehall Glacier (dark red, Sinclair et al., 2012), TALDICE (blue, Stenni et al., 2011), and TD96 (orange, Stenni et al., 2002). CE = Common Era; SAM = Southern Hemisphere Annular Mode; VSMOW = Vienna standard mean ocean water.

revealed rapid warming in recent decades (Barrett et al., 2009; Orsi et al., 2012; Zagorodnov et al., 2012). The muted recent warming is consistent over the Victoria Land Coast region (Figures 4a and 4b). The Antarctic-2k Victoria Land Coast temperature record (Stenni et al., 2017) lacks the recent warming signal after the mid-20th century (Figure 4a). The $\delta^{18}O_{ice}$ and δD_{ice} records from the ice cores in northern Victoria Land show no evidence of warming since the mid-20th century (Figure 4b). The lack of a warming signal in recent decades was also observed in the nearby automated weather system (AWS) records. We used the hourly temperature record from the seven AWSs located within 100 km from Styx Glacier (Figure S9). The average of the annual mean temperature records from the seven AWSs shows no warming trend since 1988 CE (Figure 2b; trend = −0.1 ± 0.6 °C per decade, F stat = 0.70, p = 0.41). In addition, the global reanalysis-based Antarctic temperature reconstruction ($RECON_{CFSR}$) demonstrates an insignificant temperature trend around Victoria Land over 1958–2012 CE (Nicholas & Bromwich, 2014). The mean annual temperature of $RECON_{CFSR}$ at Styx Glacier also shows statistically insignificant temperature slope (0.0 ± 0.1 °C per decade, F stat = 0.63, p = 0.43) over the 1958–2012 CE interval (Figure 2b). All of these lines of evidence indicate that there has been no significant warming in recent decades in northern Victoria Land.

3.2. Influence of SAM on Styx Glacier Temperatures

To explore the mechanism for the lack of warming in Styx Glacier since the mid-1950s, we used $RECON_{CFSR}$ temperature fields (Nicholas & Bromwich, 2014) because they have longer time series and are less biased

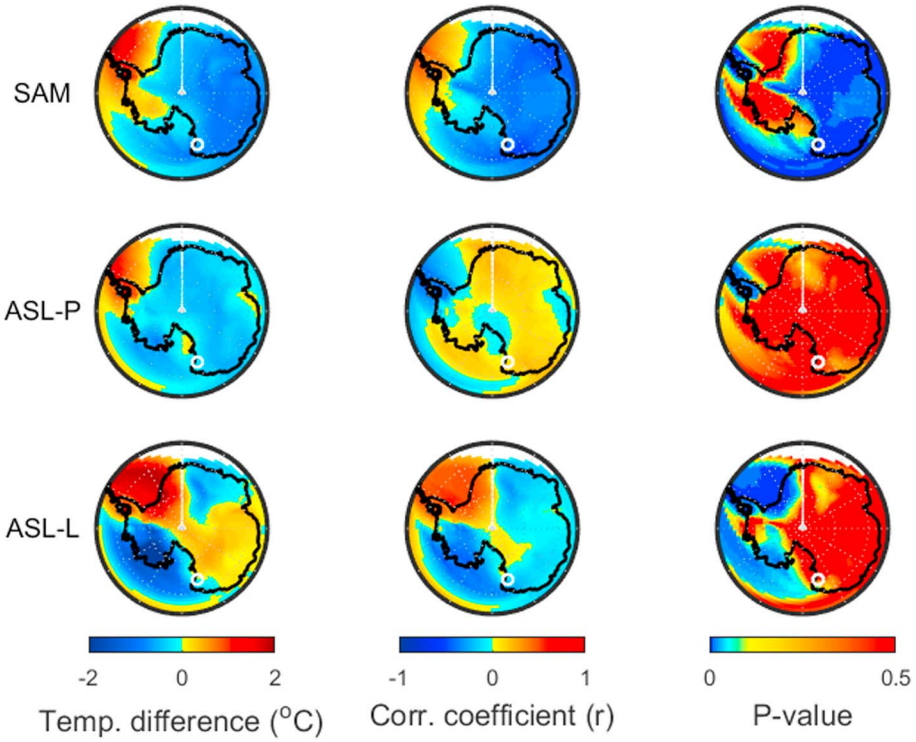

Figure 5. Influence of SAM (top row), ASL-P (middle row), and ASL-L (bottom row) on Antarctic temperatures. (left column) Difference in annual mean $RECON_{CFSR}$ temperatures between the years when each index was in both polarities. (middle column) Pearson's correlation coefficients between the annual mean $RECON_{CFSR}$ temperatures and each index. (right column) The *p* values of the correlation. The Styx Glacier borehole location is denoted as a white open circle.
SAM = Southern Hemisphere Annular Mode; ASL-P = actual center pressure of the Amundsen-Bellingshausen Sea Low; ASL-L = longitude of the Amundsen-Bellingshausen Sea Low position.

than the reanalysis; they also have a very proximal grid point (73°46.55′S, 163°13.14′E) to Styx Glacier. We calculated the composite difference of temperature at Styx Glacier according to the state of SAM and ASL change. Here we used the annual SAM index (Marshall, 2003), the actual center pressure of the ASL (ASL-P hereafter), and the longitude of the ASL position (ASL-L hereafter; Hosking et al., 2016). The annual SAM index is available since 1957 CE, while the ASL-P and ASL-L indices start in 1979 CE. First, we selected the years where the annual SAM index was higher (more positive) and lower (more negative) than the 1σ range from the mean of the entire data. Then, we calculated the difference between the annual mean temperatures of $RECON_{CFSR}$ fields at Styx Glacier between the years of more positive SAM and those of more negative SAM. An identical procedure was applied for the ASL-P and ASL-L indices. It should be noted that, in case of the ASL-P, the temperature difference was calculated by subtracting the higher ASL-P (weaker ASL) temperatures from the lower ASL-P (stronger ASL) temperatures (Figure 5). We found statistically significant (Student's *t* test at 95%) cooling of 0.6 °C at Styx Glacier when SAM was in the positive phase. In contrast, we observed no statistically significant temperature change with the changing ASL-P and ASL-L. Furthermore, we observe that the annual mean $RECON_{CFSR}$ temperature at Styx Glacier shows a statistically significant negative correlation with the annual SAM index ($r = -0.46$, $p < 0.0005$), indicating that the SAM explains ~21% of the variance. The observed negative correlation with SAM is consistent with previous results (e.g., Marshall, 2007; Nicholas & Bromwich, 2014), although the correlation is not strong. Meanwhile, no statistically significant correlations are found in the comparisons with ASL-P and ASL-L.

4. Discussion

The proxy-based SAM reconstruction data (SAM_{RECON}) seem to be related to the Styx Glacier temperatures before the mid-20th century. The SAM_{RECON} records were calculated by using temperature reconstructions

from the James Ross Island ice core along with the South American and Antarctic temperature records (Abram et al., 2014). The SAM_{RECON} records show a positive trend from the mid-17th century to ~1800 CE, followed by a negative trend from the early 19th century to ~1940 CE, after which the trend becomes significantly positive (Abram et al., 2014). The Styx Glacier temperatures exhibit increases during the negative slopes of SAM_{RECON} (yellow shading in Figure 4a) and insignificant changes when the SAM_{RECON} shows a positive slope (blue shadings in Figure 4a). Given that climate trends similar to those at the Styx Glacier are observed in Hercules Névé (Figure 4b), this implies that the influence of SAM might have been persistent in this region since before the 20th century.

The trend toward the positive phase of SAM in recent decades has been attributed to stratospheric ozone depletion and anthropogenic greenhouse gas (GHG) emissions (Abram et al., 2014; Gillett & Fyfe, 2013; Thompson et al., 2011). In the future, the expected ozone recovery (e.g., Kuttippurath & Nair, 2017; Solomon et al., 2016) may lead to a negative shift of SAM, but increasing GHG emissions might counteract the SAM shift due to the ozone recovery, likely causing SAM to stay in the positive phase (e.g., Myhre et al., 2013; Thompson et al., 2011). If the relationship between SAM and the Styx Glacier climate presented in this study persists, then the future climate in this region will depend on the degree of stratospheric ozone recovery and anthropogenic GHG emissions.

5. Conclusions

In this study, we provide the first borehole thermometry record in northern Victoria Land that extends back to the 19th century. According to our results, the surface temperature at Styx Glacier during the 20th century is 1.7 ± 0.4 °C higher than the long-term average over the 17–19th centuries. Warming since the 19th century is also found in the $\delta^{18}O_{ice}$ records from Hercules Névé, which implies that this warming occurs around the eastern coast of northern Victoria Land. In contrast, temperatures at Styx Glacier exhibit no significant increase since the mid-20th century. The ice cores in northern Victoria Land and the nearby AWS records both exhibit no evidence of warming in the last six decades, indicating a large-scale phenomenon in northern Victoria Land. The climate trends at the Styx Glacier might be related to changes in the SAM phase since before the 20th century.

Acknowledgments
We thank Howard Conway and Christo Buizert for helpful discussions. This study was supported by Korea Meteorological Administration Research and Development grant (KMIPA 2015-6080), Korea Polar Research Institute (PE 18040), and National Research Foundation of Korea (NRF-2018R1A2B3003256 and NRF-2018R1A5A1024958). The AWS data were obtained from the "Meteo-Climatological Observatory at Mario Zucchelli Station and Victoria Land" of Programma Nazionale di Ricerche in Antartide (www.climantartide.it). The data sets supporting this study are given in the supporting information.

References

Abram, N. J., Mulvaney, R., Vimeux, F., Phipps, S. J., Turner, J., & England, M. H. (2014). Evolution of the Southern Annular Mode during the past millennium. *Nature Climate Change*, *4*(7), 564–569. https://doi.org/10.1038/nclimate2235

Alley, R. B., & Koci, B. R. (1990). Recent warming in central Greenland? *Annals of Glaciology*, *14*, 6–8. https://doi.org/10.3189/S0260305500008144

Arrigo, K. R., & van Dijken, G. L. (2003). Phytoplankton dynamics within 37 Antarctic coastal polynya systems. *Journal of Geophysical Research*, *108*(C8), 3271. https://doi.org/10.1029/2002JC001739

Barrett, B. E., Nicholls, K. W., Murray, T., Smith, A. M., & Vaughan, D. G. (2009). Rapid recent warming on Rutford Ice Stream, West Antarctica, from borehole thermometry. *Geophysical Research Letters*, *36*, L02708. https://doi.org/10.1029/2008GL036369

Blunier, T., Spahni, R., Barnola, J.-M., Chappellaz, J., Loulergue, L., & Schwander, J. (2007). Synchronization of ice core records via atmospheric gases. *Climate of the Past*, *3*(2), 325–330. https://doi.org/10.5194/cp-3-325-2007

Buizert, C., Cuffey, K. M., Severinghaus, J. P., Baggenstos, D., Fudge, T. J., Steig, E. J., et al. (2015). The WAIS Divide deep ice core WD2014 chronology—Part 1: Methane synchronization (68-31 ka BP) and the gas age-ice age difference. *Climate of the Past*, *11*(2), 153–173. https://doi.org/10.5194/cp-11-153-201

Buizert, C., Martinerie, P., Petrenko, V. V., Severinghaus, J. P., Trudinger, C. M., Witrant, E., et al. (2012). Gas transport in firn: Multiple-tracer characterization and model intercomparison for NEEM, Northern Greenland. *Atmospheric Chemistry and Physics*, *12*(9), 4259–4277. https://doi.org/10.5194/acp-12-4259-2012

Clow, G. D., Saltus, R. W., & Waddington, E. D. (1996). A new high-precision borehole-temperature logging system used at GISP2, Greenland, and Taylor Dome, Antarctica. *Journal of Glaciology*, *42*(142), 576–584. https://doi.org/10.3189/S0022143000003555

Collins, M., Knutti, R., Arblaster, J., Dufresne, J.-L., Fichefet, T., Friedlingstein, P., et al. (2013). Long-term climate change: Projections, commitments and irreversibility. In *Climate change 2013: The physical science basis. Contribution of Working Group I to the Fifth Assessment Report of the Intergovernmental Panel on Climate Change* (pp. 1029–1136). Cambridge: Cambridge University Press.

Comiso, J. C., Gersten, R. A., Stock, L. V., Turner, J., Perez, G. J., & Cho, K. (2017). Positive trend in the Antarctic sea ice cover and associated changes in surface temperature. *Journal of Climate*, *30*(6), 2251–2267. https://doi.org/10.1175/JCLI-D-16-0408.1

Dansgaard, W., & Johnsen, S. J. (1969). A flow model and a time scale for the ice core from Camp Century, Greenland. *Journal of Glaciology*, *8*(53), 215–223. https://doi.org/10.3189/S0022143000031208

Fogt, R. L., & Wovrosh, A. J. (2015). The relative influence of tropical sea surface temperatures and radiative forcing on the Amundsen Sea Low. *Journal of Climate*, *28*(21), 8540–8555. https://doi.org/10.1175/JCLI-D-15-0091.1

Fretwell, P., Pritchard, H. D., Vaughan, D. G., Bamber, J., Barrand, N., Bell, R., et al. (2013). Bedmap2: Improved ice bed, surface and thickness datasets for Antarctica. *The Cryosphere*, *7*(1), 375–393. https://doi.org/10.5194/tc-7-375-2013

Gillett, N. P., & Fyfe, J. C. (2013). Annular mode changes in the CMIP5 simulations. *Geophysical Research Letters*, *40*, 1189–1193. https://doi.org/10.1002/grl.50249

Goursaud, S., Masson-Delmotte, V., Favier, V., Orsi, A., & Werner, M. (2018). Water stable isotope spatio-temporal variability in Antarctica in 1960–2013: Observations and simulations from the ECHAM5-wiso atmospheric general circulation model. *Climate of the Past*, *14*(6), 923–946. https://doi.org/10.5194/cp-14-923-2018

Greene, C. A., Gwyther, D. E., & Blankenship, D. D. (2017). Antarctic Mapping Tools for MATLAB. *Computers & Geosciences*, *104*, 151–157. https://doi.org/10.1016/j.cageo.2016.08.003

Han, Y., Jun, S. J., Miyahara, M., Lee, H. G., Ahn, J., Chung, J. W., et al. (2015). Shallow ice-core drilling on Styx glacier, northern Victoria Land, Antarctica in the 2014-2015 summer. *Journal of the Geological Society of Korea*, *51*(3), 343–355. https://doi.org/10.14770/jgsk.2015.51.3.343

Herron, M. M., & Langway, C. C. (1980). Firn densification: An empirical model. *Journal of Glaciology*, *25*(93), 373–385. https://doi.org/10.3189/S0022143000015239

Hosking, J. S., Orr, A., Bracegirdle, T. J., & Turner, J. (2016). Future circulation changes off West Antarctica: Sensitivity of the Amundsen Sea Low to projected anthropogenic forcing. *Geophysical Research Letters*, *43*, 367–376. https://doi.org/10.1002/2015GL067143

Hosking, J. S., Orr, A., Marshall, G. J., Turner, J., & Phillips, T. (2013). The influence of the Amundsen-Bellingshausen Seas Low on the climate of West Antarctica and its representation in couples climate model simulations. *Journal of Climate*, *26*(17), 6633–6648. https://doi.org/10.1175/JCLI-D-12-00813.1

Hur, S. D. (2013). *Development of core technology for ice core drilling and ice core bank* (Rep. BSPE13070–037-7). Incheon: Korea Polar Research Institute.

Jacobs, S. S. (2004). Bottom water production and its links with the thermohaline circulation. *Antarctic Science*, *16*(4), 427–437. https://doi.org/10.1017/S095410200400224X

Kuttippurath, J., & Nair, P. J. (2017). The signs of Antarctic ozone hole recovery. *Scientific Reports*, *7*(1), 585. https://doi.org/10.1038/s41598-017-00722-7

Marshall, G. J. (2003). Trends in the Southern Annular Mode from observations and reanalyses. *Journal of Climate*, *16*(24), 4134–4143. https://doi.org/10.1175/1520-0442(2003)016<4134:TITSAM>2.0.CO;2

Marshall, G. J. (2007). Half-century seasonal relationships between the Southern Annular Mode and Antarctic temperatures. *International Journal of Climatology*, *27*(3), 373–383. https://doi.org/10.1002/joc.1407

Maule, C. F., Purucker, M. E., Olsen, N., & Mosegaard, K. (2005). Heat flux anomalies in Antarctica revealed by satellite magnetic data. *Science*, *309*(5733), 464–467. https://doi.org/10.1126/science.1106888

Mitchell, L. E., Brook, E. J., Lee, J. E., Buizert, C., & Sowers, T. (2013). Constraints on the Late Holocene anthropogenic contribution to the atmospheric methane budget. *Science*, *342*(6161), 964–966. https://doi.org/10.1126/science.1238920

Mitchell, L. E., Brook, E. J., Sowers, T., McConnell, J. R., & Taylor, K. (2011). Multidecadal variability of atmospheric methane, 1000-1800 C.E. *Journal of Geophysical Research*, *116*, G02007. https://doi.org/10.1029/2010JG001441

Muto, A., Scambos, T. A., Steffen, K., Slater, A. G., & Clow, G. D. (2011).Recent surface temperature trends in the interior of East Antarctica from borehole frin temperature measurements and geophysical inverse methods. *Geophysical Research Letters*, *38*, L15502. https://doi.org/10.1029/2011GL048086

Myhre, G., Shindell, D., Bréon, F.-M., Collins, W., Fuglestvedt, J., Huang, J., et al. (2013). Anthropogenic and natural radiative forcing. In *Climate change 2013: The physical science basis. Contribution of Working Group I to the Fifth Assessment Report of the Intergovernmental Panel on Climate Change* (pp. 659–740). Cambridge: Cambridge University Press.

Nicholas, J. P., & Bromwich, D. H. (2014). New reconstruction of Antarctic near-surface temperatures: Multidecadal trends and reliability of global reanalyses. *Journal of Climate*, *27*(21), 8070–8093. https://doi.org/10.1175/JCLI-D-13-00733.1

Nye, J. F. (1963). Correction factor for accumulation measured by the thickness of the annual layers in an ice sheet. *Journal of Glaciology*, *4*(36), 785–788. https://doi.org/10.3189/S0022143000028367

Orsi, A. J., Cornuelle, B. D., & Severinghaus, J. P. (2012). Little Ice Age cold interval in West Antarctica: Evidence from borehole temperature at the West Antarctic Ice Sheet (WAIS) Divide. *Geophysical Research Letters*, *39*, L09710. https://doi.org/10.1029/2012GL051260

Orsi, A. J., Cornuelle, B. D., & Severinghaus, J. P. (2014). Magnitude and temporal evolution of Dansgaard-Oeschger event 8 abrupt temperature change inferred from nitrogen and argon isotopes in GISP2 ice using a new least-squares inversion. *Earth and Planetary Science Letters*, *395*, 81–90. https://doi.org/10.1016/j.epsl.2014.03.030

Orsi, A. J., Kawamura, K., Masson-Delmotte, V., Fettweis, X., Box, J. E., Dahl-Jensen, D., et al. (2017). The recent warming trend in North Greenland. *Geophysical Research Letters*, *44*, 6235–6243. https://doi.org/10.1002/2016GL072212

Schneider, D. P., Deser, C., & Okumura, Y. (2012). An assessment and interpretation of the observed warming of West Antarctica in the austral spring. *Climate Dynamics*, *38*(1–2), 323–347. https://doi.org/10.1007/s00382-010-0985-x

Shapiro, N. M., & Ritzwoller, M. H. (2004). Inferring surface heat flux distributions guided by a global seismic model: Particular application to Antarctica. *Earth and Planetary Science Letters*, *223*(1–2), 213–224. https://doi.org/10.1016/j.epsl.2004.04.011

Sinclair, K. E., Bertler, N. A. N., & van Ommen, T. D. (2012). Twentieth-Century surface temperature trends in the Western Ross Sea, Antarctica: Evidence from a high-resolution ice core. *Climate Dynamics*, *25*, 3629–3636. https://doi.org/10.1175/JCLI–D–11–00496.1

Sinclair, K. E., Bertler, N. A. N., Bowen, M. M., & Arrigo, K. R. (2014). Twentieth century sea-ice trends in the Ross Sea from a high-resolution, coastal ice-core record. *Geophysical Research Letters*, *41*, 3510–3516. https://doi.org/10.1002/2014GL059821

Solomon, S., Ivy, D. J., Kinnison, D., Mills, M. J., Neely, R. R., & Schmidt, A. (2016). Emergence of healing in the Antarctic ozone layer. *Science*, *353*(6296), 269–274. https://doi.org/10.1126/science.aae0061

Stenni, B., Buiron, D., Frezzotti, M., Albani, S., Barbante, C., Bard, E., et al. (2011). Expression of the bipolar see-saw in Antarctic climate records during the last deglaciation. *Nature Geoscience*, *4*(1), 46–49. https://doi.org/10.1038/NGEO1026

Stenni, B., Caprioli, R., Cimino, L., Cremisini, C., Flora, O., Gragnani, R., et al. (1999). 200 years of isotope and chemical records in a firn core from Hercules Névé, northern Victoria Land, Antarctica. *Annals of Glaciology*, *29*, 106–112. https://doi.org/10.3189/172756499781821175

Stenni, B., Curran, M. A. J., Abram, N. J., Orsi, A., Goursaud, S., Masson-Delmotte, V., et al. (2017). Antarctic climate variability on regional and continental scales over the last 2000 years. *Climate of the Past*, *13*(11), 1609–1634. https://doi.org/10.5194/cp-13-1609-2017

Stenni, B., Proposito, M., Gragnani, R., Flora, O., Jouzel, J., Falourd, S., & Frezzotti, M. (2002). Eight centuries of volcanic signal and climate change at Talos Dome (East Antarctica). *Journal of Geophysical Research*, *107*(D9), 4076. https://doi.org/10.1029/2000JD000317

Stieg, E. J., Schneider, D. P., Rutherford, C. D., Mann, M. E., Comiso, J. C., & Shindell, D. T. (2009). Warming of the Antarctic ice-sheet surface since the 1957 International Geophysical Year. *Nature*, *457*(7228), 459–462. https://doi.org/10.1038/nature07669

Thompson, D. W. J., Solomon, S., Kushner, P. J., England, M. H., Grise, K. M., & Karoly, D. J. (2011). Signatures of the Antarctic ozone hole in Southern Hemisphere surface climate change. *Nature Geoscience*, *4*(11), 741–749. https://doi.org/10.1038/ngeo01296

Yang, J.-W., Ahn, J., Brook, E. J., & Ryu, Y. (2017). Atmospheric methane control mechanisms during the early Holocene. *Climate of the Past*, *13*(9), 1227–1242. https://doi.org/10.5194/cp-13-1227-2017

Yen, Y. C. (1981). *Review of thermal properties of snow, ice and sea ice* (Rep. 81–10). Hanover: United States Army Cold Region Research and Engineering Lab.

Zagorodnov, V., Nagornov, O., Scambos, T. A., Muto, A., Mosley-Thompson, E., Pettit, E. C., & Tyuflin, S. (2012). Borehole temperatures reveal details of 20th century warming at Bruce Plateau, Antarctic Peninsula. *The Cryosphere*, *6*(3), 675–686. https://doi.org/10.5194/tc-6-675-2012